Макрогетероциклы
http://macroheterocycles.isuct.ru

DOI: 10.6060/mhc190127b

An Influence of Copper Cation in the Complex on Structure of the Nanostructured Layers, Spectral and Electrocatalytic Characteristics of Langmuir–Schaeffer Films of Triphenylcorrole

Nadezhda M. Berezina,[a@1] Thao T. Vu,[b] Nadezhda V. Kharitonova,[a] Larisa A. Maiorova,[a@2] Oskar I. Koifman,[a,c] and Sergei V. Zyablov[d]

Dedicated to Prof. Dieter Wöhrle on the occasion of his Birthday

[a]*Institute of Macroheterocyclic Compounds, Ivanovo State University of Chemistry and Technology, 153000 Ivanovo, Russian Federation*
[b]*National University, Hanoi, Vietnam*
[c]*G.A. Krestov Institute of Solution Chemistry, Russian Academy of Sciences, 153045 Ivanovo, Russian Federation*
[d]*Profi-studio, 153037 Ivanovo, Russian Federation*
[@1]*Corresponding author E-mail: sky_berezina@rambler.ru*
[@2]*Corresponding author E-mail: maiorova.larissa@gmail.com*

An influence of copper cation in the complex on structure and properties of the floating layers of 5,10,15-triphenylcorrole (Cu[(ms-Ph)$_3$Cor]) at the air-water interface was studied. The structure of the layers has been determined using the method of quantitative analysis of compression isotherms. A model of stable nanostructured layers of the substance has been constructed. Copper cation in the macrocycle increases the density of two-dimensional M-nanoaggregates, while the number of molecules in such aggregates experiences 2–3-fold growth. Like the metal-free triphenylcorrole, this copper-containing compound in multilayer Langmuir-Schaeffer (LS) films with edge-on arrangement of molecules forms aggregates with strong intermolecular interactions. Such LS films may be suitable for electrocatalysis in the oxygen reduction reaction.

Keywords: Copper 5,10,15-triphenylcorrole, compression isotherms, nanostructured layers, M-nanostructures, Langmuir-Schaefer films, UV-Vis spectra, electrocatalysis.

Влияние катиона меди в составе комплекса на структуру наноструктурированных слоев, спектральные и электрокаталитические характеристики пленок Ленгмюра–Шефера трифенилкоррола

Н. М. Березина,[a1] Ву Тхи Тхао,[b] Н. В. Харитонова,[a] Л. А. Майорова,[a2] О. И. Койфман,[a,c] С. В. Зяблов[d]

[a]*Институт макрогетероциклических соединений, Ивановский государственный химико-технологический университет, 153000 Иваново, Российская Федерация*
[b]*Национальный университет, Ханой, Вьетнам*
[c]*Институт химии растворов им. Г.А. Крестова РАН, 153045 Иваново, Российская Федерация*
[d]*ООО Профи-студия, 153037 Иваново, Российская Федерация*

Исследовано влияние катиона меди в составе комплекса на структуру и свойства плавающих слоев 5,10,15-трифенилкоррола (Cu[(ms-Ph)$_3$Cor]) на границе раздела вода-воздух. С помощью метода количественного анализа изотерм сжатия определена структура и построена модель наноструктурированных плавающих слоев Cu[(ms-Ph)$_3$Cor]. Установлено, что введение катиона металла в полость макроцикла приводит к повышению

плотности формируемых в слое двумерных М-наноагрегатов и значительному (в 2–3 раза) увеличению числа молекул в них. Трифенилкоррол меди, аналогично безметальному трифенилкорролу, в полислоевых пленках Ленгмюра-Шефера (ЛШ) с edge-on расположением молекул формирует агрегаты с сильными межмолекулярными взаимодействиями. ЛШ-пленки коррола могут быть использованы в качестве материалов для электрокатализа в реакции электровосстановления кислорода.

Ключевые слова: 5,10,15-Трифенилкоррол меди, изотермы сжатия, наноструктурированные слои, М-наноструктуры, пленки Ленгмюра-Шефера, электронная спектроскопия, электрокатализ.

Introduction

Macroheterocyclic compounds are able to form organic nanostructures due to the self assembly.[1–4] Self-assembly of porphyrins and related compounds is one of the dominant concepts in the development of functional systems based on this class of compounds.[5–7] The creation of thin-film of organic materials, consisting of two- and three-dimensional nanoparticles is of great interest.[8,9] The Langmuir-Blodgett technology makes it possible to solve such problems.[10–13] A specific feature of macroheterocyclic compounds in confined space – in floating layers, thin films and in capsules is the ability to form aggregates, whose properties may differ from the properties of these compounds in solutions.[14–17] It was shown that porphyrins and their derivatives are capable to form stable *M* (Major)-nanoaggregates 5–20 nm in size at the air-water interface.[18–21] In our previous studies we demonstrated that the supramolecular design with controlled self-organization of organic compounds in 2D and 3D nanostructures at the air-water interface becomes possible if quantitative information about the structure of the floating layer is available. The quantitative method for analyzing of compression isotherms of floating layers allows determination of the critical characteristics of the layers. It was shown that the equation describing a nanostructured monolayer at the liquid/gas interface has the form: $\pi(A - A_{mol}) = n^{-1}kT$.[17] Here π is surface pressure, A is area per molecule in monolayer, A_{mol} is the area per molecule in the nanoaggregate, n is aggregation number. Later, it was used to determine the number of molecules in aggregates of the crown-phthalocyanine ligand on the surface of water and by other authors.[22]

Thin films of corroles possess peculiar structural and photophysical properties, making them candidates for application as photosensitizers, electronic molecular devices, *etc*.[23–26] Corroles (H_3Cor) compared to porphyrins (H_2P), have a wider variety of macrocyclic structures and high reactivity.[27–33] Corrole has the ability to stabilize high oxidation states of the central metal atoms such as Cr^{V}, Mn^{IV}, Fe^{IV}, Co^{IV}, Cu^{III} being a trianionic ligand.[34] Due to their structural and electronic features, corroles are perspective compounds for their use as active components of catalytic systems[35] for various redox processes, groups transfer reactions, molecular recognition processes for small molecules.[36] The films of germanium methoxy-triphenylcorrole were obtained and studied by atomic force microscopy using the matrix pulse laser evaporation technology.[25] It was shown that the Soret and *Q*-bands are broadened and shifted in the UV-Vis spectra of films. That was explained by the presence of a high degree of aggregation during deposition of the films from the [(*p*-MeO-Ph)$_3$Cor]Ge solution. In the UV-Vis spectra of Cu(*p*-MeO-Ph)$_3$Cor films[37] obtained by evaporation of the solvent, a bathochromic shift of the Soret band is observed (by 15 nm) compared with the spectrum of the Cu(*p*-MeO-Ph)$_3$Cor solution in dichloromethane. Such peculiarities of the films are caused by formation of *J*-aggregates. Corroles with bulk substituents form *H*-aggregates. Absorption spectra of the films have the differences with respect to the spectra of the solutions. The Soret bands are shifted into the blue region (by 20 nm). In the films intermolecular distances increase. Two-dimensional nanostructures of organic compounds are of interest for creating nanomaterials with new properties.[38–42] The self-assembly of the two- and three-dimensional nanostructures of corroles was shown earlier.[43–47] Spontaneous self-assembly mostly operates through weak intermolecular forces, such as hydrogen bonding, alkyl chain packing, π–π interactions which dictate the formation of nanostructures.

The oxygen reduction reaction (ORR) is an important reaction not only *in vivo* tissue respiration processes, but also in many electrochemical technologies, including the operation of a hydrogen-oxygen fuel cell,[48] chlorine-alkaline electrolysis with air-depolarized cathodes,[49,50] metal-air batteries,[51] electrochemical sensors.[52,53] Most of the works were devoted to studies of the catalytic activity of metallocomplexes deposited on the electrode surface, for example, graphite or carbon material. Such a principle has used in fuel cells.[52–57] In particular, in the works on electrocatalysis of cobalt corroles,[58–62] it was shown that the rate and mechanism of the ORR were influenced by the chemical structure of the catalyst molecule, the nature of the central metal ion in the molecule, *etc*.

It was shown earlier that corroles are able to form nanostructured floating mono- and multilayers at the air-water interface.[63,64] The influence of various factors on the structure of the floating layers of corroles was described. The effect of the initial surface coverage on the structure of the floating layers of 5,10,15-triphenylcorrole (H_3[(*ms*-Ph)$_3$Cor])[53] and effect of temperature of subphase on the layers of manganese(III) 7,13-dimethyl-2,3,8,12,17,18-hexamethylcorrole was demonstrated.[35] However, the influence of a metal cation on the quantitative characteristics (such as size of nanoaggregates, the number of molecules in nanoaggregates, density of nanoaggregates) has not yet been studied.

The objectives of this work are (1) to discover the conditions and to obtain monomolecular nanostructured floating layers of copper 5,10,15-triphenylcorrole (Cu[(*ms*-Ph)$_3$Cor]); (2) to determine the main characteristics of *M*-monolayers; (3) to develop a model and to create a passport of floating

monolayers; (4) to study the effect of the copper on the structure of the floating layers of triphenylcorrole; (5) to form Langmuir-Schaefer (LS) films of Cu[(*ms*-Ph)$_3$Cor]; (6) to study the spectral characteristics and catalytic activity of LS films of triphenylcorrole and its complex with copper in the oxygen reduction reaction.

Experimental

Copper 5,10,15-triphenylcorrole (Cu[(*ms*-Ph)$_3$Cor]) was synthesized by the known procedure.[53,63,65] The compound was identified using the methods of UV-Vis, NMR spectroscopy and MALDI-TOF mass spectrometry.

To obtain the floating layers the solution of Cu[(*ms*-Ph)$_3$Cor] in dichloromethane (C=1.2·10^{-4} M) was applied onto the surface of bidistilled water with a microliter syringe (Hamilton, Sweden) at the temperature of 20±1 °C. The volume of the solution to be applied was determined according to the required initial surface coverage degree (c_{face}), *i.e.* the ratio of the area occupied by the molecules of the substance to the total area of water surface available to the molecules. Two percentage values of the initial surface coverage degree were calculated for two extreme orientations of molecules: the c_{face}, assuming that planes of all the molecules of the substance are parallel to water surface (the molecules lie "face-on"), and the c_{edge}, assuming the planes are orthogonal to the surface (the molecules stand "edge-on"). Fifteen minutes after the application of the solution the layer was compressed at a rate of v = 2.3 cm^2·min^{-1}. Floating layers in this work were formed at c_{face}/c_{edge} values from 4/2.5 to 93/58 %. The experiment was carried out on the "NT-MDT" installation (Zelenograd, Russia). The surface pressure was measured by Wilhelmy sensor (with an accuracy of 0.02 mN/m).

Langmuir-Schaefer (LS) films of 5,10,15-triphenylcorrole and its copper complex were prepared by deposition of floating layers at onto quartz substrates and at onto carbon-graphite electrodes at the temperature of 20±1 °C. While compressing the layer on the water surface, barriers of the Langmuir trough were stopped when the selected pressure was reached; then the layers were transferred one by one onto the substrate using the horizontal lift method. The number K of touchdowns of the layer by the substrate is 15. The layers for transfer onto quartz substrates were formed at c_{face}/c_{edge} of 93/58 %. Electron absorption spectra of LS films and solution were recorded with a Shimadzu-UV-1800 spectrophotometer (the wavelength error was ±1 nm).

Electrochemical measurements were performed by the cyclic voltammetry in the three-electrode cell YASE-2. The measurements were carried out by using the potentiostat-galvanostat «J-31P». A carbon-graphite electrode was used as a working electrode, the lateral surface was isolated by a fluoroplastic shell. The working surface (0.64 cm^2) was deposited with a layer (0.2–0.3 mm) of an active mass, which was prepared in an ethyl alcohol, involved the carbon support (TEC – technical elemental carbon P-514 (state standard 7885-86) with the ash content 0.45 %), the fluoroplastic suspension (6 % FP-4D) and LS film. While studying redox reactions occurring on electrodes involving the active mass, first of all, electrolyte deaeration of argon (99.99 %) was conducted by bubbling for 40 min. Next, the working electrode was dipped in the electrolyte and cyclic voltammograms were recorded in the potential range of 0.5–1.5 V. Then, gaseous oxygen was introduced into the electrolyte, and *I,E*-curves were recorded in the same potential range. The correlations between current density (j) and the electrode potential were plotted for a comparative analysis of the LS films electrocatalytic activity. Oxygen or argon was fed into the electrolyte from cylinders by sparging at a rate (0.14 ml·s^{-1}) through a gearbox with a fine adjustment valve and a glass capillary. After of the experiment, the layer of active mass was easily removed, and the operation of applying a new layer could be repeated many times.

The structure of the layers at air-water interface was analyzed using quantitative analysis of compression isotherms of a nanostructured *M*-monolayer, based on the concept of a layer as a real two-dimensional gas with structural elements representing two dimensional nanoaggregates. A method for the quantitative analysis of compression isotherms and the determination of the main characteristics of a nanostructured *M*-monolayer are described in detail in the works.[17,67–69] The area (A) per molecule in the layer was determined with 2 % error. The maximum error values for other characteristics are as follows: 3 % for surface area per molecule in a nanoaggregate (A_{mol}) and the pressure region where the stable state exists, and the span of the region ($\Delta\pi$); 5 % for initial surface coverage degrees (c_{face}), the average distance between molecules in the aggregate (r) and the lowest tilt angle of molecules in stacks ("dry" aggregates, ψ); 6 % for surface area of a nanoaggregate (S_{aggr}); 7 % for diameter of a nanoaggregate (D_{aggr}) and water content between *M*-aggregates (per molecule) at the initial point of the stable state ($w_{inter\text{-}M\text{-}i}$); 10 % for compressibility of the layer (B), surface coverage degrees at the initial and final points of the stable state $c_{i\text{-}face(edge)}$, $c_{f\text{-}face(edge)}$, surface coverage degree by *M*-aggregates at the initial point of the stable state ($c_{i\text{-}aggr}$), aggregation number (n), density of the aggregate (ρ_{aggr}), water content in *M*-aggregates ($w_{in\text{-}M}$), and the distance between nanoaggregates at initial points of the stable state (d_i).

The geometric parameters of the molecule are as follows: projection areas $A_{proj(face)}$ = 1.6 nm^2, $A_{proj(edge)}$ = 1 nm^2; areas of circumscribed rectangles $A_{rec(face)}$ = 3.2 nm^2 and $A_{rec(edge)}$ = 1.4 nm^2 (Figure 1). The areas per molecule in the closest-packed monolayer are $A_{pack(face)}$ = 1.9 nm^2 and $A_{pack(edge)}$ = 1.2 nm^2 (the HyperChem 8.0.8 software package (PM3 calculation method).

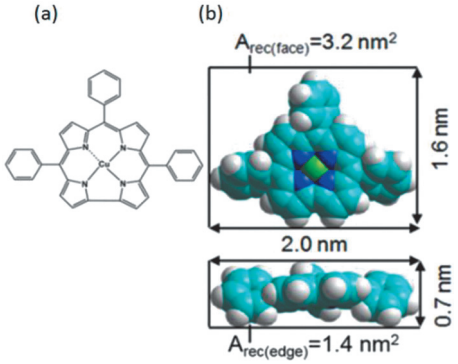

Figure 1. Copper 5,10,15-triphenylcorrole: the structural formula (a) and the spatial model (b) with sizes and areas of circumscribed rectangles (A_{rec}).

Results and Discussion

It was shown earlier that metal free 5,10,15-triphenylcorrole in floating at the air-water interface layers and in LS films forms stable nanostructures of different types.[53,63–64,66] In this work, the structure and properties of floating layers of copper 5,10,15-triphenylcorrole at the air-water interface in a wide range of initial surface coverage degrees (c_{face}/c_{edge} from 4/2.5 % to 93/58 %, Figure 2) were studied.

A quantitative analysis of compression isotherms built in the πA–π axes (Figure 2b) shows that at low surface pressures (up to 0.3–1.6 mN/m) stable Cu[(*ms*-Ph)$_3$Cor]

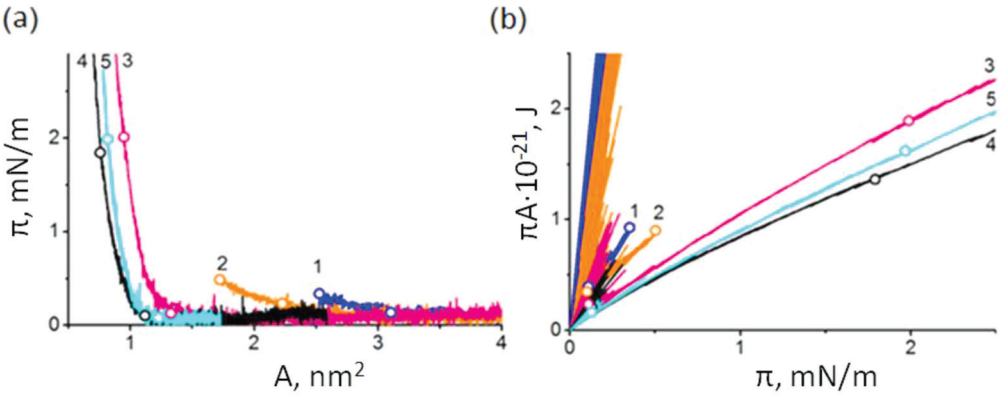

Figure 2. Frames enlarged low-pressure region of the π–*A* (a) and π*A*–π (b) compression isotherms of floating layers of Cu[(*ms*-Ph)$_3$Cor]. The isotherms were recorded for different initial surface coverage degrees 10/6 % (1), 14/9 % (2), 37/23 % (3), 62/39 % (4), 93/58 % (5). White circles denote regions corresponding to the stable monolayers.

Table 1. Characteristics of Cu[(*ms*-Ph)$_3$Cor] floating layers, formed at different initial surface coverage degrees.

c_{face} (c_{edge}) (%)	Nanoaggregate type	$c_{i\text{-}face}$-$c_{f\text{-}face}$ ($\Delta c_{j\text{-}face}$) (%)	$c_{i\text{-}aggr}$ (%)	π_i-π_f (mN/m)	A_{mol} (nm^2)	n	D_{aggr} (S_{aggr}) (nm) (nm^2)	ψ_{min} (°)	r (nm)	$w_{in\text{-}M}/A_{mol}$ ρ_{aggr} (%)	$w_{inter\text{-}M\text{-}i}$ (nm^2)	d_i (nm)	B (m/N)
Cu[(*ms*-Ph)$_3$Cor], C= 1.2·10^{-4} M, CH_2Cl_2													
4 (2.5)	Monolayer M_{face}	21–25 (4)	76	0.1–0.4	5.70	14	10 (80)	0	1.3	72 (0.28)	1.80	1.5	480
7 (4.4)		37–46 (9)	80	0.1–0.4	3.43	40	13 (140)	0	0.7	53 (0.47)	0.87	1.6	620
10 (6)		52–60 (8)	83	0.1–0.4	2.54	67	15 (170)	0	0.4	37 (0.63)	0.51	1.4	440
12 (8)		64–72 (8)	84	0.1–0.3	2.10	96	16 (200)	0	0.2	24 (0.76)	0.40	1.5	440
14 (9)	Monolayer M_{edge}	76–92 (16)	71	0.1–0.5	1.50	27	7 (40)	53*	–	20$^{\Delta}$ (–)	0.60	1.3	420
16 (10)		96–113 (17)	80	0.1–0.4	1.33	45	9 (60)	64*	–	10$^{\Delta}$ (–)	0.34	1.1	510
18 (11)		103–123 (20)	81	0.1–0.3	1.25	81	11 (100)	72*	–	5$^{\Delta}$ (–)	0.29	1.2	640
20 (13)		109–128 (19)	84	0.1–0.3	1.23	117	14 (144)	77*	–	3$^{\Delta}$ (–)	0.24	1.3	610
24 (15)		110–133 (23)	84	0.1–0.4	1.22	162	16 (200)	80*	–	2$^{\Delta}$ (–)	0.23	1.4	480
31 (19)	Bilayer M_{bi}	107–172 (65)	59	0.1–1.4	0.87	48	5 (20)	–	–	0	0.63	1.6	300
37 (23)		119–168 (49)	67	0.1–1.3	0.90	57	6 (30)	–	–	0	0.45	1.4	240
62 (39)		135–208 (73)	72	0.1–1.4	0.85	75	7 (40)	–	–	0	0.33	1.3	260
74 (46)		130–182 (52)	72	0.1–1.6	0.89	81	7 (40)	–	–	0	0.34	1.2	190
93 (58)		145–193 (48)	68	0.1–1.5	0.90	112	8 (50)	–	–	0	0.26	0.8	180

c_{face}/c_{edge} face-on and edge-on are initial surface coverage degrees; $c_{i\,(face,\,edge)}$ and $c_{f\,(face,\,edge)}$ are surface coverage degrees at the initial and final points of the stable state, respectively; $\Delta c_{j\text{-}face}$ is span of surface coverage degree, region where the state exists; $c_{i\text{-}aggr}$ is surface coverage degree by *M*-aggregates at the initial point of the stable state; π_i–π_f is the pressure region where the stable state exists, and the span of the region; A_{mol} is surface area per molecule in a nanoaggregate; *n* is aggregation number (the number of molecules in an aggregate); D_{aggr} and S_{aggr} are diameter and surface area of a nanoaggregate; ψ_{min} is the lowest tilt angle of molecules in stacks ("dry" aggregates); *r* is the average distance between molecules in the aggregate; $w_{in\text{-}M}/A_{mol}$ and $w_{inter\text{-}M\text{-}i}$ are water content in *M*-aggregates and between them (per molecule) at the initial point of the stable state; ρ_{aggr} is density of the aggregate; d_i is the distance between nanoaggregates at initial points of the stable state; *B* is compressibility of the layer.

$^{\Delta}$ the amount of water in the aggregates was calculated for vertical arrangement of the molecules in the stacks.

nanostructures of different types are formed. It was established that Cu[(*ms*-Ph)$_3$Cor] forms 3 types of stable floating layers: face-on monolayers, edge-on monolayers and edge-on bilayers. Characteristics of floating layers of are presented in Table 1.

At low initial surface coverage degrees (c_{face}/c_{edge} from 4/2.5 % to 12/8 %), face-on monolayers of Cu[(*ms*-Ph)$_3$Cor] where molecules in nanoaggregates are parallel to the water surface are formed. Such monolayers are characterized by large values of the area per molecule in nanoaggregates (A_{mol} from 5.7 to 2.1 nm^2). The number of molecules (n) in the aggregates increases from 14 to 96 with an increase in the initial surface coverage degree. In addition, with an increase of c_{face}, the aggregates become larger (D_{aggr} from 10 nm to 16 nm), the density of aggregates increases (ρ_{aggr} from 0.28 to 0.76).

At medium surface coverage degree (from 14/9 % to 24/15 %) and low surface pressure (from 0.1 to 0.5 mN/m),

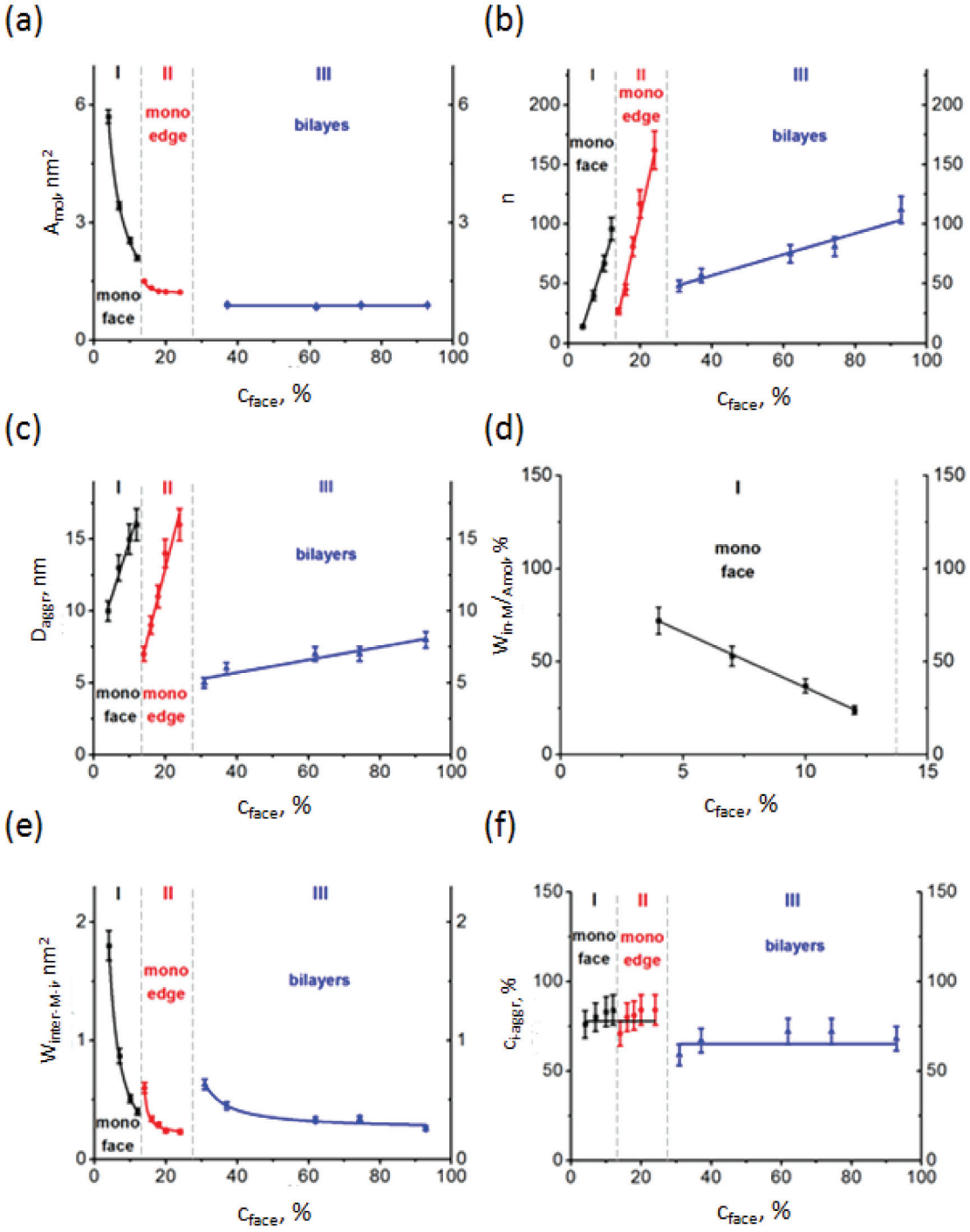

Figure 3. The dependencies on the initial surface coverage degree for: the area per molecule in *M*-aggregate (A_{mol}, a), the aggregation number (n, b), the diameter of *M*-nanoaggregates (D_{aggr}, c), the content of water in nanoaggregates (w_{in-M}/A_{mol}, d), content of water between nanoaggregates ($w_{inter-Mi-i}$ per molecule, e) and the surface coverage degree by *M*-aggregates (c_{i-aggr}, f). For graphs (e) and (f) the values are determined at the initial and final points of the stable state, respectively. Vertical dashed lines show the boundaries between layers of different types.

stable edge-on monolayers where molecules in nanoaggregates are tilted to the water surface are formed. The lowest tilt angle in stacks of Cu[(*ms*-Ph)$_3$Cor] molecules (ψ_{min}) varies from 53 to 80°, the number of molecules in M_{edge}-aggregates is from 27 to 162.

Monolayers of face-on and edge-on types are characterized by a high value of compressibility (420–640 m/N). A specific feature of monolayers of copper 5,10,15-triphenylcorrole is the independence of the degree of surface coverage by *M*-aggregates at the start point of a stable state ($c_{i\text{-}aggr}$ = 78 %) on the initial surface coverage degree and monolayer state.

At high initial surface covering degrees in a very wide range of c_{face}/c_{edge} (from 31/19 % to 93/58 %), stable bilayers in the region of low pressures (from 0.1 to 1.6 mN/m) are formed. For monolayers with face-on and edge-on arrangement of molecules in nanoaggregates and for bilayers, the dependences of all the characteristics of the layers on the initial surface coverage degree were determined. The dependencies on the initial surface coverage for surface area per molecule in a *M*-aggregate, the number of molecules in an aggregate, diameter of a *M*-nanoaggregates, water content in nanoaggregates, water content between a nanoaggregates (per molecule) and surface coverage by *M*-aggregates are shown in Figure 3.

Dependencies of characteristics of the layer on the initial surface coverage degree result in the following equations:

For M_{face} monolayers:

$A_{mol} = 100/(2.7 + 3.7 \cdot c_{face})$ (1),

$n = -23.4 + 9.3 \cdot c_{face}$ (2),

$D_{aggr} = 7.1 + 0.8 \cdot c_{face}$ (3),

$w_{in\text{-}M}/A_{mol} = 95.6 - 5.9 \cdot c_{face}$ (4),

$w_{inter\text{-}M\text{-}i} = 1/(-0.4 + 0.2 \cdot c_{face})$ (5),

$c_{i\text{-}aggr}$ = 78 % (6),

$r = 1.56 - 0.11 \cdot c_{face}$ (7),

$c_{i\text{-}face} = -0.2 + 5.3 \cdot c_{face}$ (8),

$c_{f\text{-}face} = 1.9 + 5.9 \cdot c_{face}$ (9).

For M_{edge} monolayers:

$A_{mol} = 1.18 + 0.39/(c_{face} - 12.79)$ (10),

$n = -161.4 + 13.3 \cdot c_{face}$ (11),

$D_{aggr} = -6.53 + 0.97 \cdot c_{face}$ (12),

$w_{inter\text{-}M\text{-}i} = 0.2 + 0.3/(c_{face} - 13.2)$ (13),

$c_{i\text{-}aggr}$ = 78 % (14),

$\psi_{min} = 15.0 + 2.8 \cdot c_{face}$ (15),

$c_{i\text{-}face} = 32.7 + 3.5 \cdot c_{face}$ (16),

$c_{f\text{-}face} = 39.3 + 4.2 \cdot c_{face}$ (17).

For M_{bi} 3D-layers:

A_{mol} = 0.9 nm^2 (18),

$n = 21.6 + 0.9 \cdot c_{face}$ (19),

$D_{aggr} = 3.93 + 0.04 \cdot c_{face}$ (20),

$W_{inter\text{-}M\text{-}i} = 0.3 + 2.4/(c_{face} - 24.6)$ (21),

$c_{i\text{-}aggr}$ = 65 % (22).

The equations (1–22) and the basic equation of state of the monolayer – $\pi(A - A_{mol}) = kT/n$, form a model of floating monolayers of copper 5,10,15-triphenylcorrole.

The boundaries between the layers of different types were determined: $c_{bord\_face\text{-}edge}$ = 13.5 ± 0.4 (%); $c_{bord\_edge\text{-}bi}$ = 27.5 ± 0.8 (%).

Table 2.* The passport of floating layers of Cu[(*ms*-Ph)$_3$Cor] ($C = 1.2 \cdot 10^{-4}$ M, CH_2Cl_2; v =2.3 cm^2·min^{-1}; t=20±1 °C).

Nanoaggregate type	Orientation of molecules in a *M*-aggregate	Formation conditions, c_{face}(%) (from the model)	Dependences of characteristics of a monolayer on c_{face} (from the model)	Constants characterizing the floating layers (from the model)
2D, M_{face}	face-on	$c_{face} \le 13.1$	$n = -23.4 + 9.3 \cdot c_{face}$ $D_{aggr} = 7.1 + 0.8 \cdot c_{face}$ $w_{in\text{-}M}/A_{mol} = 95.6 - 5.9 \cdot c_{face}$ $w_{inter\ M\text{-}i} = 1/(-0.4 + 0.2 \cdot c_{face})$ $r = 1.56 - 0.11 \cdot c_{face}$ $c_{i\text{-}face} = -0.2 + 5.3 \cdot c_{face}$ $c_{f\text{-}face} = 1.9 + 5.9 \cdot c_{face}$ $c_{i\text{-}aggr}$ = const (78 %)	$n^{max} = 98$ $(D_{aggr})^{max}$ = 18 nm $(w_{in\text{-}M}/A_{mol})^{min}$ = 18 % $(w_{inter\ M\text{-}i})^{min}$ = 0.4 nm r^{min} = 0.1 nm $(c_{i\text{-}face})^{max}$ = 69 % $(c_{f\text{-}face})^{max}$ = 79 % $c_{i\text{-}aggr}^{const}$ = 78 %
2D, M_{edge}	edge-on	$13.9 \le c_{face} \le 26.7$	$n = -161.4 + 13.3 \cdot c_{face}$ $D_{aggr} = -6.53 + 0.97 \cdot c_{face}$ $w_{inter\ M\text{-}i} = 0.2 + 0.3/(c_{face} - 13.2)$ $\psi_{min} = 15.0 + 2.8 \cdot c_{face}$ $c_{i\text{-}face} = 32.7 + 3.5 \cdot c_{face}$ $c_{f\text{-}face} = 39.3 + 4.2 \cdot c_{face}$ $c_{i\text{-}aggr}$ = const (78 %)	$n^{max} = 193$ $(D_{aggr})^{max}$ = 19 nm $(w_{inter\ M\text{-}i})^{min}$ = 0.2 nm $(\psi_{min})^{max} = 90^0$ $(c_{i\text{-}face})^{max}$ = 126 % $(c_{f\text{-}face})^{max}$ = 151 % $c_{i\text{-}aggr}^{const}$ = 78 %
3D, M_{Bi}	edge-on	$c_{face} \ge 28.3$	A_{mol} = const (0.9 nm^2) $n = 21.6 + 0.9 \cdot c_{face}$ $D_{aggr} = 3.93 + 0.04 \cdot c_{face}$ $w_{inter\ M\text{-}i} = 0.25 + 2.4/(c_{face} - 24.6)$ $c_{i\text{-}aggr}$ = const (65 %)	$n^{min} = 47$ $(D_{aggr})^{min}$ = 5.2 nm $(w_{inter\ M\text{-}i})^{max}$ = 0.9 nm $(w_{inter\ M\text{-}i})^{min}$ = 0.25 nm $c_{i\text{-}aggr}^{const}$ = 65 %

*Notations see under Table 1.

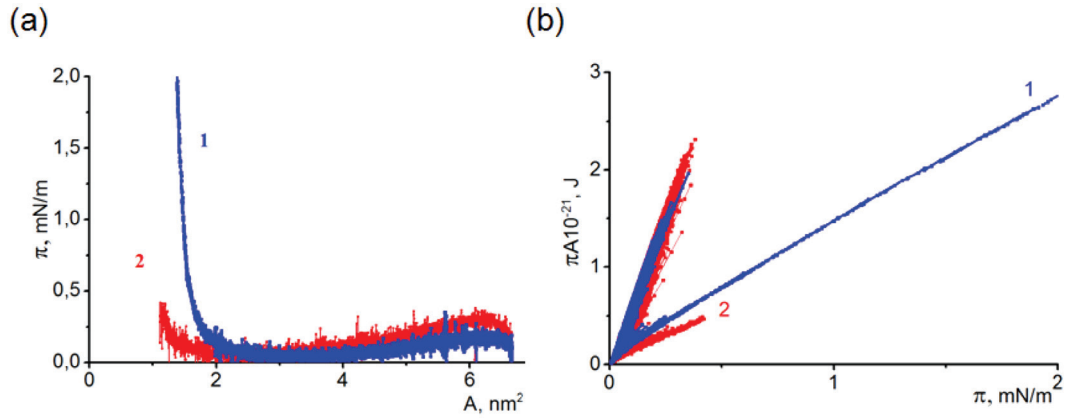

Figure 4. π-*A* (a) and π*A*-π (b) – Compression isotherms of floating layers of H_3[(*ms*-Ph)$_3$Cor] (1) and Cu[(*ms*-Ph)$_3$Cor] (2), at c_{face} = 24 % (C = 1.2·10^{-4} M, CH_2Cl_2).

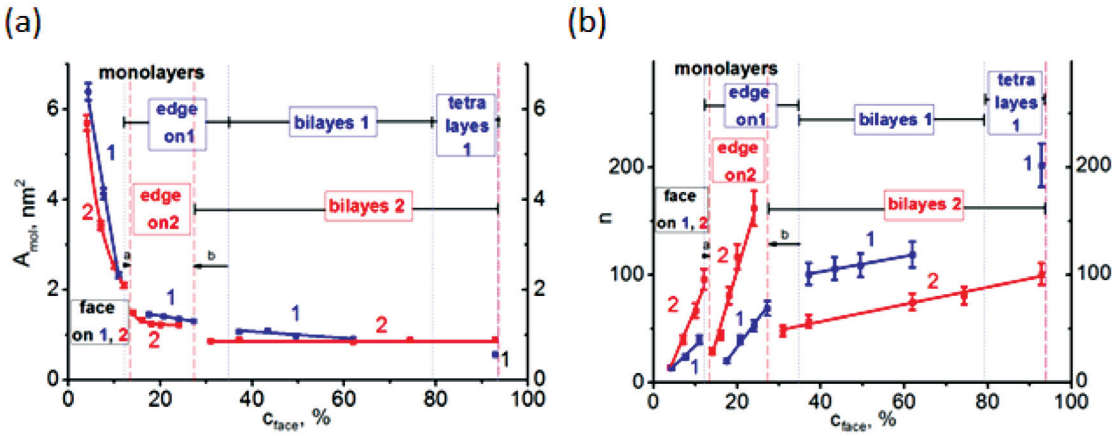

Figure 5. The dependencies on the initial surface coverage degree for: the area per molecule in *M*-aggregate (A_{mol}, a), the aggregation number (*n*, b) in H_3[(*ms*-Ph)$_3$Cor] (1) and Cu[(*ms*-Ph)$_3$Cor] (2) layers. Vertical dashed lines show the boundaries between layers of different types.

From the equations (1–22), taking into account boundary values, the constants characterizing floating face-on and edge-on monolayers as well as bilayers were determined: the maximum number of molecules in the nanoaggregates, the diameter and the area of the aggregate, minimal water content inside and between nanoaggregates, to name a few. These constants, along with the conditions for formation of monolayers of various types and the dependence of the characteristics of the layer on initial surface coverage degree, are presented in the passport of Cu[(*ms*-Ph)$_3$Cor] floating layers (Table 2).

Figure 4 demonstrates the effect of the copper atom on the triphenylcorrole isotherms at c_{face}/c_{edge} = 24/15 %.

A comparison of the main characteristics (A_{mol} and *n*) of nanostructured layers of the compounds on initial surface coverage degree is shown in Figure 5.

It is follows that a ligand of triphenylcorrole, at c_{face}/c_{edge} > 79/50 % and at pressure up 0 to 2.2 mN/m, forms tetralayers, in contrast to its complex with copper, which forms bilayers. The region of the stable edge-on monolayers for the ligand is 9 % larger in the initial surface coverage degree than for the complex with copper (Figure 5). It is shown that nanoaggregates of the complex more dense than nanoaggregates of the ligand (Figure 5a). The number of molecules in Cu[(*ms*-Ph)$_3$Cor] aggregates more than the number of molecules in H_3[(*ms*-Ph)$_3$Cor] aggregates (by 2–3 times, Figure 5b). The rate of change the number of molecules in face-on and edge-on nanoaggregates with increasing of the initial surface coverage degree is 2–3 times greater for the complex than for the ligand (Figure 5b). The monolayers of the ligand and the complex are characterized by a constant value of $c_{i\text{-}aggr}$ (76 %). The specific feature of monolayers of the copper complex (with face-on and edge-on arrangements of molecules) is stability of the monolayers only at very low pressures (up to 0.4–0.5 mN/m). The monolayers of ligand are stable up to 2.2 mN/m.[60]

Schematic views of floating monolayers and 3D nanoaggregates of triphenylcorrole and its complex with copper formed at different initial surface coverage degrees are shown in Figure 6.

The formed floating layers were transferred onto the substrates (quartz and surface of the electrodes) by the horizontal lift method. The pressures and states

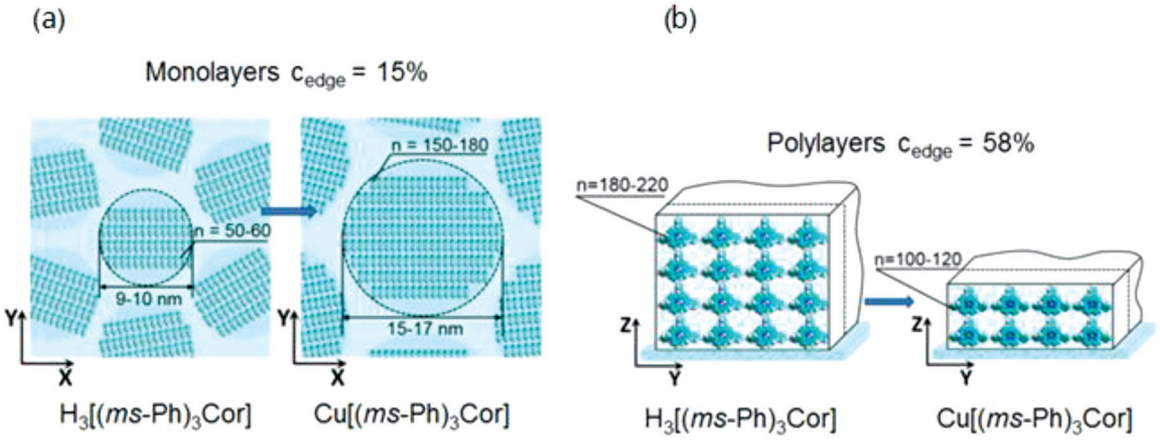

Figure 6. Schematic views of fragments of floating monolayers (a) and 3D nanoaggregates (b) of triphenylcorrole and its copper complex, formed at the same conditions (c_{edge} = 15 %, a, and c_{edge} = 58 %, b).

of floating layers at which they were transferred to the substrates are shown in Figure 7. The layer state in the A point was estimated from the coordinates of the point.

The state of the Cu[(*ms*-Ph)$_3$Cor] layer at the point A corresponds to «edge-on bilayer – tetralayer» (samples I and II, Figure 7). The state of the H_3[(*ms*-Ph)$_3$Cor] layer at the point B corresponds to «edge-on tetralayer» (sample III, Figure 7). Figure 8a shows the absorption spectra of solution in CH_2Cl_2 and LS films of Cu[(*ms*-Ph)$_3$Cor].

It is shown that the main band, both in solution and in film, consists of two bands: (1 sol) 406 nm and (2 sol) 411 nm, (1 film) 404 nm and (2 film) 420 nm, respectively (Figure 8). The position of right shoulder of solution (sh sol) is 440 nm. The position of right shoulder of film (sh film) is 438 nm. The ratios of intensity of the bands for the solution are I (1)/I (2) = 1.5 and I (1)/I (sh) = 4.6. The ratios of intensity of the bands for the film are I (1)/I (2) = 7.8 and I (1)/I (sh) = 1.9. The ratios of the half-widths of the bands for the film and solution are FWHM (1 film)/FWHM (1 sol) = 1.2, FWHM (2 film)/FWHM (2 sol) = 0.9, FWHM (sh film)/FWHM (sh sol) = 1.9. The main difference the spectrum of LS film compared with the spectrum of solution is the bathochromic shift by 9 nm and a significant decrease in the ratio of intensity of the second main band and the first one. The *Q*-bands are red shifted (Figure 8a). In addition, the shoulder of the film is more intense with respect to the first main band, and wider than the shoulder of solution. Thus, the Cu[(*ms*-Ph)$_3$Cor], as well as the ligand, in the film forms aggregates with strong intermolecular interactions.[63,70,71]

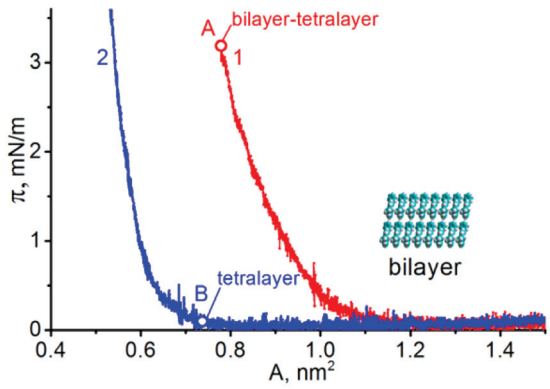

Figure 7. π-*A* – Compression isotherms of floating layers of Cu[(*ms*-Ph)$_3$Cor] (1, c_{edge} = 58 %) and H_3[(*ms*-Ph)$_3$Cor] (2, c_{edge} 58 %). Points A and B indicate the pressure at which the layers were transferred to the substrate. The state of the Cu[(*ms*-Ph)$_3$Cor] layer at the point A corresponds to «edge-on bilayer – tetralayer» (samples I and II). The state of the H_3[(*ms*-Ph)$_3$Cor] layer at the point B corresponds to «edge-on tetralayer» (sample III).

In order to study the catalytic activity of copper triphenylcorrole LS films and its ligand in the ORR, 15 layers of H_3[(*ms*-Ph)$_3$Cor] were transferred (isotherm 1, point A, the state of the layer "bilayer-tetralayer", sample 2) and Cu[(*ms*-Ph)$_3$Cor] (isotherm 2, point B, the state of the layer edge-on "tetralayer", sample 3, Figure 7) on the surface of carbon-graphite electrodes through a thin layer of TEC-based composite material. For a comparative analysis of the electrocatalytic activity of the LS films, *I,E*-curves, corresponding to the saturation of the electrolyte with oxygen (40 minutes), were obtained. The dependence of the current density of ORR on the potentials of the electrode containing carbon material and LS films (Figure 8b) shows that, compared with TEC ($E_{1/2}(O_2)$ = –0.30 V), when only 15 layers of triphenylcorrole ligand were applied (thickness was about 80 nm) or a copper complex (thickness was about 60 nm), a depolarization effect was observed, which manifests itself in the displacement of the half-wave potential $E_{1/2}(O_2)$ towards positive values for the ligand ($E_{1/2}(O_2)$ = –0.29 V) and complex ($E_{1/2}(O_2)$ = –0.28 V). Thus, it was shown that LS films of corroles can be used as materials for electrocatalysis.

Conclusion

The aggregation behavior of copper 5,10,15-triphenylcorrole in layers at the water surface and in LS films was studied. It is shown that at the different initial surface coverage degrees, 2D and 3D nanostructures of Cu[(*ms*-Ph)$_3$Cor] are formed at the air-water interface. The conditions of the formation of nanostructures were determined: face-on monolayers are formed at $c_{face} \leq$ 13.1 %, edge-on monolayers

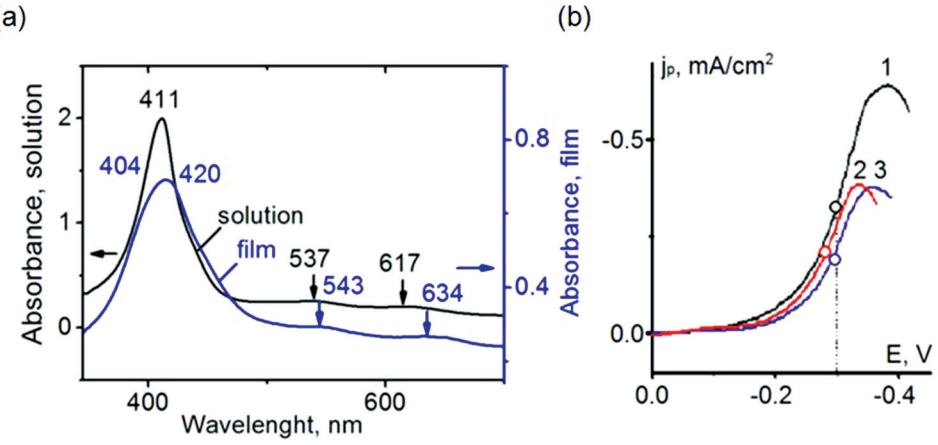

Figure 8. (a) UV-Vis spectra of Cu[(*ms*-Ph)$_3$Cor] in CH_2Cl_2 solution (C = 1.2·10^{-4} M) and LS film (sample I); (b) current density of the ORR as a function of electrode potential with various catalysts: 1 – TEC, 2 – 15 layers of Cu[(*ms*-Ph)$_3$Cor] (sample II), 3 – 15 layers of H_3[(*ms*-Ph)$_3$Cor] (sample III).

are formed at 13.9 % ≤ c_{face} ≤ 26.7 %, and edge-on bilayers are formed at c_{face} ≥ 28.3 %. It was shown that the range of formation of stable bilayers of copper 5,10,15-triphenylcorrole is very wide (from c_{face} 31 % to c_{face} 93 %). The main characteristics of *M*-monolayers (the size of nanoaggregates, the number of molecules in the aggregate, the distances between the aggregates, *etc*.) were determined. The dependencies of characteristics of the layer on the initial surface coverage degree were determined. A model of floating layers of Cu[(*ms*-Ph)$_3$Cor] was constructed and a passport the layers was compiled.

It was determined that the introduction of a copper into the macrocycle cavity leads to an increase in the density of two-dimensional *M*-nanoaggregates and a significant (by 2–3 times) increase in the number of molecules in them. Face-on and edge-on monolayers of the copper complex, unlike the ligand, are stable only at very low pressures (up to 0.4–0.5 mN/m). At high initial surface coverage degree under same conditions, the complex with copper forms bilayers, unlike H_3[(*ms*-Ph)$_3$Cor] which forms tetralayers. The surface coverage degree by *M*-aggregates at the initial point of a stable state of copper triphenylcorrole, as well as the ligand, does not depends on the initial surface coverage degree and the arrangement of molecules in the aggregates.

It was shown that both copper triphenylcorrole and the ligand, in multilayer LS films form nanoaggregates with strong intermolecular interactions. The possibility to use such LS films for electrocatalysis in the oxygen reduction reaction has been demonstrated.

Acknowledgments. This work has been supported by the government task of the Ministry of Education and Science of the Russian Federation (4.1929.2018/4.6).

References

1. Liu H., Xu J., Li Y., Li Y. *Acc. Chem. Res.* **2010**, *43*, 1496−1508.
2. Ariga K., Hill J.P., Lee M.V. *Sci. Technol. Adv. Mater.* **2008**, *9*, 1–96.
3. Maiorova L.A., Kobayashi N., Zyablov S.V., Bykov V.A., Nesterov S.I. *Langmuir* **2018**, *34*, 9322−9329.
4. Valkova L., Borovkov N., Pisani M., Rustichelli F. *Thin Solid Films* **2001**, *401*, 267−272.
5. Satake A., Kobuke Y. *Tetrahedron* **2005**, *61*, 13–41.
6. Karlyuk M.V., Krygin Y.Y., Maiorova L.A., Ageeva T.A., Koifman O.I. *Russ. Chem. Bull.* **2013**, *62*, 471–479.
7. Konev D.V., Lizgina K.V., Zyubina T.S., Zyubin A.S., Vorotyntsev M.A. *Electrochim. Acta* **2014**, *122*, 3−10.
8. Valkova L.A., Betrencourt C., Hochapfel A., Myagkov I.V., Feigin L.A. *Mol. Cryst. Liq. Cryst.* **1996**, *287*, 269–273.
9. Petrova M.V., Maiorova L.A., Bulkina T.A., Ageeva T.A., Koifman O.I., Gromova O.A. *Macroheterocycles* **2014**, *7*, 267−271.
10. Ariga K., Nishikawa M., Mori T., Takeya J., Shrestha L.K., Hill J.P. *Sci. Technol. Adv. Mater.* **2019**, *20*, 51–95.
11. Lettieri R., Monti D., Zelenka K., Trnka T., Drašar P., Venanzi M. *New J. Chem.* **2012**, *36*, 1246.
12. Valkova L.A., Glibin A.S., Valli L., Casilli S., Giancane G. *Langmuir* **2008**, *24*, 4857−4864.
13. Valkova L., Borovkov N., Koifman O., Kutepov A., Berzina T. *Biosens. Bioelectron.* **2004**, *20*, 1177−1184.
14. Maiorova L.A., Erokhina S.I., Pisani M. *Colloids Surf., B: Biointerfaces* **2019**, *182*, 110366.
15. Akopova O.B., Bronnikova A.A., Kruvchinskii A. *J. Struct. Chem.* **1998**, *39*, 376−383.
16. Valkova L.A., Shabyshev L.S., Borovkov N.Yu., Feigin L.A., Rustichelli F. *J. Inclusion Phenom. Macrocyclic Chem.* **1999**, *35*, 243−249.
17. Valkova L.A., Glibin A.S., Valli L. *Colloid J.* **2008**, *70*, 6–11.
18. Stoffelen C., Huskens J. *Small* **2016**, *12*, 96−119.
19. Maiorova L.A., Koifman O.I. In: *Functional Materials Based on Tetrapyrrole Macroheterocyclic Compounds* (Koifman O.I., Ed.) Moscow: URSS, **2019**. Ch. 18, p. 701–740 (in Russ.) [Майорова Л.А., Койфман О.И. В кн.: *Функциональные материалы на основе тетрапиррольных макрогетероциклических соединений* (Койфман О.И., ред.) М.: URSS, **2019**. Глава 18, с. 701–740].
20. Kharitonova N.V., Maiorova L.A., Koifman O.I. *J. Porphyrins Phthalocyanines* **2018**, *22*, 509–520.
21. Valkova L.A., Glibin A.S., Koifman O.I., Erokhin V.V. *J. Porphyrins Phthalocyanines* **2011**, *15*, 1044−1051.
22. Shokurov A.V., Selektor S.L., Arslanov V.V., Karpacheva M.I., Gagina I.A. *Macroheterocycles* **2012**, *5*, 358−365.

23. Wang Y., Akhigbe J., Ding Y., Bruckner Ch., Lei Y. *Electroanalysis* **2012**, *24*, 1348–1355.
24. Blondeau Patissier V., Vanotti M., Prêtre T., Rabus D., Tortora L., Barbe J.M., Ballandras S. *Procedia Engineering* **2011**, *25*, 1085–1088.
25. Caricato A.P., Lomascolo M., Luches A., Mandoj F., Manera M.G. *Appl. Phys. A* **2008**, *93*, 651–654.
26. Bursa B., Wróbel D., Lewandowska K., Graja A., Grzybowski M., Gryko D.T. *Synth. Met.* **2013**, *176*, 18–25.
27. Aviv I., Gross Z. *Chem. Eur. J.* **2009**, *15*, 8382–8394.
28. Aviv I., Gross Z. *Coord. Chem. Rev.* **2011**, *255*, 717–736.
29. Karimov D.R. Synthesis, Spectral Characteristics and Reactivity of Corroles with Different Types of Functional Substitution. PhD Diss., Ivanovo, **2011**. 159 p. (in Russ.).
30. Palmer J.H. *Struct. Bond.* **2012**, *142*, 49–90.
31. Liu H.-Y., Mahmood M. HR, Qiu Sh.-X., Chang Ch.K. *Coord. Chem. Rev.* **2013**, *257*, 1306–1333.
32. Barata J.F.B., Santos C.I.M., Grac M., Neves P.M.S., Faustino M.A.F., Cavaleiro J.A.S. *Top. Heterocycl. Chem*. **2013**, *33*, 79–141.
33. Thomas K.E., Alemayehu A.B., Conradie J., Beavers CH.M., Ghosh A. *Acc. Chem. Res*. **2012**, *45*, 1203–1214.
34. Meier-Callahan A.E., Gray H.B., Gross Z. *Inorg. Chem*. **2000**, *39*, 3605–3607.
35. Paolesse R., Natale C.D., Macagnano A., Sagone F., Scarselli M.A., Chiaradia P. *Langmuir* **1999**, *15*, 1268–1274.
36. Aviv I., Gross Z. *Chem. Commun*. **2007**, 1987−1999.
37. Gao D., Edzang J.A., Diallo A.K., Dutronc Th., Balaban T.S., Videlot-Ackermann Ch., Terazzi E., Canard G. *New J. Chem*. **2015**, *39*, 7140–7146.
38. Maiorova L.A., Koifman O.I., Burmistrov V.A., Kuvshinova S.A., Mamontov A.O. *Protec. Met. Phys. Chem. Surf.* **2015**, *51*(1), 85−92.
39. Valkova L.A., Shabyshev L.S., Feigin L.A., Akopova O.B. *Mol. Cryst. Liq. Cryst. Section C, Molecular Materials* **1996**, *6*, 291−298.
40. Topchieva I.N., Osipova S.V., Banatskaya M.I. *Doklady Akademii Nauk SSSR* **1989**, *308*(4), 910–913.
41. Valkova L.A., Shabyshev L.S., Feigin L.A., Akopova O.B. *Bulletin of the RAS. Physics* 1**997**, *61*(3), 631−636.
42. Pisani M., Maiorova L.A., Francescangeli O., Fokin D.S., Nikitin K.S. *Mol. Cryst. Liq. Cryst*. **2017**, *649*, 2–10.
43. Hameren van R., Elemans J.A.A.W., Wyrostek D., Tasior M., Gryko D.T., Rowan A.E., Nolte R.J.M. *J. Mater. Chem.* **2009**, *19*, 66–69.
44. Miao X., Gao A., Hiroto S., Shinokubo H., Osuka A., Xin H., Deng W. *Surf. Interface Anal.* **2009**, *41*, 225–230.
45. Miao X., Gao A., Li Zh., Hiroto S., Shinokubo H., Osuka A., Deng W. *Appl. Surf. Sci.* **2009**, *255*, 5885–5890.
46. Stefanelli M., Monti D., Venanzi M., Paolesse R. *New J. Chem*. **2007**, *31*, 1722–1725.
47. Lu G., Li J., Yan S., He Ch., Shi M., Zhu W., Ou Zh., Kadish K.M. *Dyes Pigm.* **2015**, *121*, 38–45.
48. Steele B.C., Heinzel A. *Nature* **2001**, *414*, 345–352.
49. Spendelow J.S., Wieckowski A. *Phys. Chem. Chem. Phys*. **2007**, *9*, 2654–2675.
50. Lipp L., Gottesfeld Sh., Chlistunoff J. *J. Appl. Electrochem*. **2005**, *35*, 1015–1024.
51. Lee J.-S., Kim S.T., Cao R., Choi N.-S., Liu M., Lee K.T., Cho J. *Adv. Energy Mater.* **2011**, *1*, 34–50.
52. Ramamoorthy R., Dutta P.K., Akbar S.A. *J. Mater. Sci*. **2003**, *38*, 4271–4282.
53. Vu T.T. Metalporphyrinoids: Stability in Solution and Solid Phase, Features, Electrocatalysis and Thin-Film Materials on Their Basis. PhD thesis, Russia, **2016**. 222 p. (in Russ).
54. Kadish K.M., Fremond L., Ou Zh., Shao J., Shi Ch., Anson F.C., Burdet F., Gros C.P., Barbe J.-M., Guilard R. *J. Am. Chem. Soc.* **2005**, *127*, 5625–5631.
55. Kadish K.M., Fremond L., Burdet F., Barbe J.-M., Gros C.P., Guilard R. J. *Inorg. Biochem*. **2006**, *100*, 858–868.
56. Collma J.P., Kaplan M., Decreau R.A. *Dalton Trans.* **2006**, *4*, 554–559.
57. Kadish K.M., Shen J., Fremond L., Chen P., El Ojaimi M. *Inorg. Chem*. **2008**, *47*, 6726–6737.
58. Schechter A., Stanevsky M., Mahammed A., Gross Z. *Inorg. Chem*. **2012**, *51*, 22–24.
59. Ou Zh., Lu A., Meng D., Huang Sh., Fang Yu., Lu G., Kadish K.M. *Inorg. Chem*. **2012**, *51*, 8890–8896.
60. Bazanov M.I., Berezina N.M., Karimov D.R., Berezin D.B. *Russ. J. Electrochem.* **2012**, *48*, 905−910.
61. Berezina N.M., Karimov D.R., Bazanov M.I., Berezin D.B. *Izv. Vyssh. Uchebn. Zaved., Ser. Khim. Khim. Tekhnol.* **2013**, *56*(6), 37−41.
62. Chang S.-T., Huang H.-Ch., Wang H.-Ch., Hsu H.-Ch., Lee J.-F., Wang Ch.-H. *Int. J. Hydrogen Energy* **2014**, *39*, 934–941.
63. Maiorova L.A., Vu T.T., Gromova O.A., Nikitin K.S., Koifman O.I. *BioNanoScience* **2018**, *8*, 81–89.
64. Vu T.T., Maiorova L.A., Berezin D.B., Koifman O.I. *Macroheterocycles* **2016**, *9*, 73–79.
65. Wasbotten I.H., Wondimagegn T., Ghosh A. *J. Am. Chem. Soc.* **2002**, *124*, 8104−8116.
66. Vu T.T., Kharitonova N.V., Maiorova L.A., Gromova O.A., Torshin I.Yu., Koifman O.I. *Macroheterocycles* **2018**, *3*, 286–292.
67. Valkova L.A., Zyablov S.V., Koifman O.I., Erokhin V.V. *J. Porphyrins Phthalocyanines* **2010**, *14*, 513−522.
68. Maiorova L.A. Controlled Self-assembling of Azaporphyrins in 2D-and 3D-nanostructures in Langmuir Layers and Langmuir- Blodgett films. D.Sc. Diss., Ivanovo, **2012**. 382 p.
69. Valkova L.A., Glibin A.S., Koifman O.I. *Macroheterocycles* **2011**, *4*, 222−226.
70. Kasha M. *Radiation Research* **1963**, *20*, 55–71.
71. de Miguel G., Hosomizu K., Umeyama T., Matano Y., Imahori H., Perez-Morales M., Martin-Romero M. T., Camacho L. *J. Colloid Interface Sci.* **2011**, *356*, 775–782.

Received 25.01.2019
Accepted 22.09.2019